

Article

# Gaseous Elemental Mercury Concentrations along the Northern Gulf of Mexico Using Passive Air Sampling, with a Comparison to Active Sampling

Byungwon Jeon <sup>1</sup>, James V. Cizdziel <sup>1,\*</sup> , J. Stephen Brewer <sup>2</sup> , Winston T. Luke <sup>3</sup>,  
Mark D. Cohen <sup>3</sup> , Xinrong Ren <sup>3,4</sup>  and Paul Kelley <sup>3,4</sup>

<sup>1</sup> Department of Chemistry and Biochemistry, University of Mississippi, University, MS 38677, USA; bjeon@go.olemiss.edu

<sup>2</sup> Department of Biology, University of Mississippi, University, MS 38677, USA; jbrewer@olemiss.edu

<sup>3</sup> Air Resources Laboratory, National Oceanic and Atmospheric Administration, College Park, MD 20740, USA; winston.luke@noaa.gov (W.T.L.); mark.cohen@noaa.gov (M.D.C.); xinrong.ren@noaa.gov (X.R.); paul.kelley@noaa.gov (P.K.)

<sup>4</sup> Department of Atmospheric and Oceanic Science, University of Maryland, College Park, MD 20742, USA

\* Correspondence: cizdziel@olemiss.edu

Received: 4 September 2020; Accepted: 23 September 2020; Published: 26 September 2020



**Abstract:** Mercury is a toxic element that is dispersed globally through the atmosphere. Accurately measuring airborne mercury concentrations aids understanding of the pollutant's sources, distribution, cycling, and trends. We deployed MerPAS<sup>®</sup> passive air samplers (PAS) for ~4 weeks during each season, from spring 2019 to winter 2020, to determine gaseous elemental mercury (GEM) levels at six locations along the northern Gulf of Mexico, where the pollutant is of particular concern due to high mercury wet deposition rates and high concentrations in local seafood. The objective was to (1) evaluate spatial and seasonal trends along the Mississippi and Alabama coast, and (2) compare active and passive sampling methods for GEM at Grand Bay National Estuarine Research Reserve, an Atmospheric Mercury Network site. We observed higher GEM levels ( $p < 0.05$ ) in the winter ( $1.53 \pm 0.03 \text{ ng m}^{-3}$ ) compared to other seasons at all sites; with the general pattern being: winter > spring > summer  $\approx$  fall. Average GEM levels (all deployment combined) were highest at Bay St. Louis ( $1.36 \pm 0.05 \text{ ng m}^{-3}$ ), the western-most site nearest the New Orleans metropolitan area, and lowest at Cedar Point ( $1.07 \pm 0.09 \text{ ng m}^{-3}$ ), a coastal marsh with extensive vegetation that can uptake GEM. The MerPAS units compared reasonably well with the established active monitoring system, but gave slightly lower concentrations, except in the winter when the two methods were statistically similar. Both the passive and active sampling methods showed the same seasonal trends and the difference between them for each season was <15%, acceptable for evaluating larger spatial and temporal trends. Overall, this work demonstrates that PASs can provide insight into GEM levels and the factors affecting them along coastal regions.

**Keywords:** atmospheric mercury; gaseous elemental mercury; passive air sampler; MerPAS<sup>®</sup>; seasonal trend; spatial trend; Gulf of Mexico; Grand Bay

## 1. Introduction

Mercury (Hg) is a persistent and toxic pollutant with a complex biogeochemical cycle, where the atmosphere plays an important role, including transport of the contaminant on local, regional, and global scales [1]. The understanding of atmospheric Hg has greatly advanced with the capability to measure gaseous elemental mercury (GEM), gaseous oxidized mercury (GOM), and particle bound mercury (PBM), the three main classes of airborne Hg species. There are challenges in accurately

measuring these species and properly interpreting the results [2–4]. GEM, the predominant form typically encompassing >95% of the total gaseous Hg, has a relatively long residence time (~6 months or more) compared to GOM and PBM (~days to weeks) [5]. Levels of each Hg species vary depending on proximity to sources, meteorological conditions, season, and other factors, with GOM and PBM levels plummeting when they are scavenged by precipitation [6,7]. GEM concentrations tend to be more stable, with background levels in the northern hemisphere about  $1.5 \text{ ng m}^{-3}$  [8]. GEM levels are decreasing at many sites in North America and Europe, likely due to the phase-out of Hg from commercial products, and increased adoption of air pollution control technologies [9]. GEM is slowly converted to PBM and highly soluble and particle-reactive GOM by photochemical and other reactions [5,6]. GOM and PBM concentrations tend to be highest near anthropogenic point sources, especially combustion sources such as coal fired power plants or waste incinerators [2,5,7]. Once deposited to terrestrial and aquatic ecosystems, Hg can be re-emitted or, given the right biogeochemical conditions, converted by certain microorganisms to methyl-Hg, a neurotoxic form that can readily accumulate in organisms and concentrate up the food chain to levels that can harm both wildlife and humans [1,6,10].

With abundant coastal wetlands that promote production and transfer of methyl-Hg into primary producers, the northern Gulf of Mexico (nGoM, a portion of the U.S. Gulf Coast extending from the Suwannee River, in the Florida panhandle, to the Sabine River, near the state line between Louisiana and Texas) is prone to Hg contaminated food webs [11]. Another factor contributing to high Hg levels along the nGoM is that the region consistently has some of the highest wet Hg deposition rates in the USA [12,13]. So, it is not surprising that levels of methyl-Hg in seafood along the nGoM exceed other U.S. coastlines, and that there are widespread fish consumption advisories in the region. This is concerning because (1) nGoM residents tend to consume more seafood than other U.S. residents, with as much as 30% of the coastal population estimated to exceed the U.S. Environmental Protection Agency's reference dose for MeHg [14], and (2) the economy of the region is intricately linked to commercial and recreational fishing. Moreover, we hypothesize that the GoM "dead-zone", a low oxygen area in the waters of the nGoM near the mouth of the Mississippi River and its spillways that occurs each summer as a result of nutrient pollution from agriculture and developed land runoff in the Mississippi River watershed, may exacerbate the Hg problem by producing conditions that favor the production of MeHg, because organic matter and low oxygen fuel certain methylating-microbes [15]. The periodic nature of the dead-zone (oxic-anoxic changes) may affect the speciation and bioavailability of Hg, which, in turn, may affect the net surface exchange of GEM with the atmosphere. Thus, it is important to measure atmospheric Hg at locations along the nGoM to help understand Hg sources, distribution, trends, and cycling in that region.

There is a relatively long record of atmospheric Hg measurements at Grand Bay National Estuarine Research Reserve (NERR) located on the eastern portion of the Mississippi coastline [16]. In addition to long-term speciated-mercury measurements, collected with an automated instrument from Tekran Instruments Corporation (hereafter just Tekran) atop a 10 m tower, along with trace gas and meteorological monitoring, research at the site has included intensive studies on atmospheric mercury speciation [17] and Hg isotopic analyses [18]. The data have provided a valuable insight on atmospheric Hg at the site, including impacts from both local and regional sources as well as large-scale Hg cycling phenomena, species-specific isotopic compositions, and diurnal and seasonal variation in Hg species. As the instrument uses active sampling, the data are temporally rich, allowing correlation with other atmospheric constituents, such as ozone and sulfur dioxide [19]. GEM depletion events have been observed in the early morning at the site, likely due to uptake by plants, and a slight GEM elevation during the day has generally been observed, likely due to downward mixing from higher concentrations aloft [16]. However, the research has been unable to directly address spatial variability in GEM concentrations because the Tekran instrument is stationary, costly, and requires power.

Passive air sampling is a low-cost no-power alternative approach to active sampling. In passive sampling the gaseous analyte enters a sampler and diffuses at a known rate through a barrier into a chamber where it is trapped on a sorbent. The sorbent is later analyzed to determine the amount of

analyte present. The airborne concentration of the analyte is calculated by dividing the mass of sorbed analyte (ng) by the deployment time (days) and the sampling rate ( $\text{m}^3 \text{ day}^{-1}$ ). Passive air samplers (PAS) are increasingly being used for studies where spatially-resolved data are needed, or where active sampling is not possible due to cost, site restrictions, such as lack of electrical power or trained operators, or other constraints [20–23]. The main advantage is that a large number of samplers can be deployed to increase area coverage and improve spatial resolution. The main limitations are that the samplers require longer periods of time to collect the analyte, limiting temporal resolution, and, specifically for atmospheric Hg, that measurements of atmospheric mercury forms other than GEM (e.g., GOM and PBM) remain challenging, although some designs have had success [24].

The MerPAS<sup>®</sup> from Tekran is a commercially available mercury passive air sampler (PAS) that traps GEM on sulfur-impregnated activated carbon and uses a diffusive barrier to constrain the sampling rate [25]. The device includes a protective shield for deployment outdoors, where it can be left to collect GEM for months without revisiting the site until it is removed for analysis. At the laboratory the sorbent is analyzed, typically with a direct mercury analyzer (DMA), and the concentrations of GEM are calculated as discussed earlier; details of the entire method and sampling rate calculations are described in Section 2.

Recent research has shown that the MerPAS<sup>®</sup> sampler can not only measure GEM but also characterize and quantify atmospheric mercury sources, both with and without isotope tracing [26,27]. We have recently shown that the MerPAS<sup>®</sup> sampler can also discriminate landscape, seasonal, and elevation effects on GEM if given sufficient collection time, adequate analytical precision, and low blank levels [28]. In the present study, we used MerPAS<sup>®</sup> units to quantify GEM at six sites along the Mississippi and Alabama Gulf Coast during four consecutive seasons, from spring 2019 to winter 2020. Herein, we report our results with emphasize on spatial and temporal trends in GEM, and a comparison between passive and active sampling data co-collected at Grand Bay NERR, a National Atmospheric Deposition Program Atmospheric Mercury Network (AMNet) site.

## 2. Material and Methods

### 2.1. Study Sites and Meteorological Measurements

GEM was determined at five locations along the Mississippi Gulf Coast, including Bay St. Louis, Gulf Port, Gulf Coast Research Laboratory (GCRL) main campus near Ocean Springs, GCRL at Cedar Point, Grand Bay NERR near Moss Point, as well as at the Dauphin Island Sea Lab located to the southeast on a barrier island in Alabama (Figure 1). Figure 1 also shows anthropogenic Hg point sources based on US Environmental Protection Agency 2018 toxic release inventory (TRI) data, the most recent TRI data available [29]. Table A1 in Appendix A provides site coordinates, sampling periods, and mean temperature and wind speed during deployment. Meteorological data stems from the nearest weather stations, ranging from on-site at Grand Bay to 4.9 km away at Bay St. Louis. The samplers were deployed for ~4 weeks during 4 consecutive seasons, starting in spring 2019. The Grand Bay site has been described in detail elsewhere [17]. Briefly, the National Oceanic and Atmospheric Administration's (NOAA's) Air Resources Laboratory established Hg monitoring at the wetland site in 2006, and has been operating Tekran systems there as part of the National Atmospheric Deposition Program's AMNet. Long-term observations of atmospheric speciated Hg at the site have been published elsewhere [16]. The Cedar City site was also within a coastal wetland, whereas the other sites were at the immediate coastline with MerPAS<sup>®</sup> units deployed above open water.

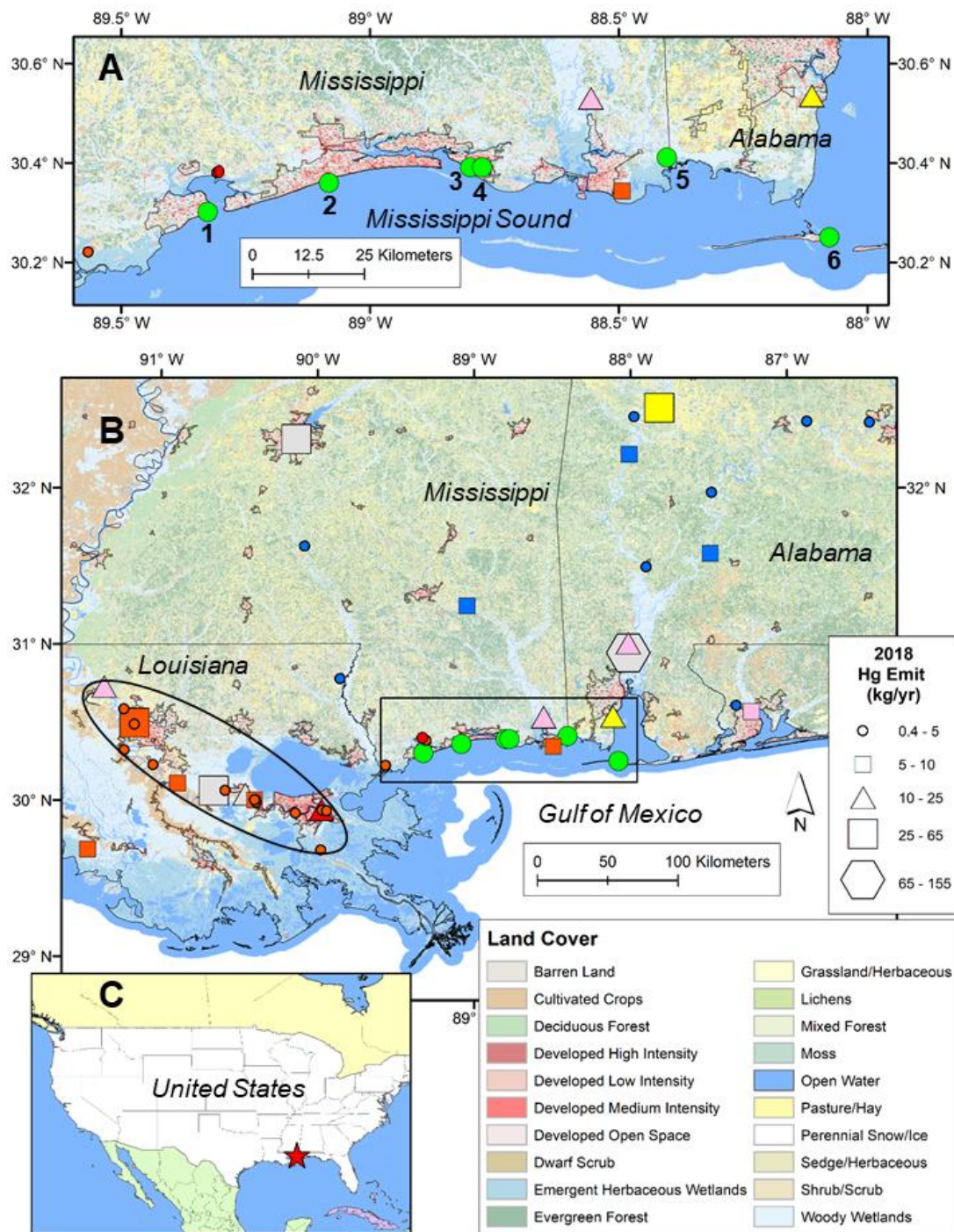


**Figure 1.** Maps of the study site. (A) = close up showing the six sampling locations as green circles (1 = Bay St. Louis; 2 = Gulfport; 3 = Gulf Coast Research Laboratory (GCRL) Main; 4 = GCRL Cedar Point; 5 = Grand Bay National Estuarine Research Reserve (NERR); 6 = Dauphin Island). (B) = a regional view with the close-up domain indicated in the box. (C) = a general location map showing the study site with star. The Hg air emission point sources are based on the most recent toxic release inventory data (2018) [29], where the size and shape of the emissions symbols indicate the amount of emissions (kg/year) and the color of the symbol indicates the source category: refineries and chemicals (red); electric power generation (pink); metals (gray); paper (blue); cement (yellow). Land cover categories are based on the 2011 National Land Cover Database [30]. The New Orleans and Baton Rouge area in Louisiana (shown with an oval) has gaseous elemental mercury (GEM) emission sources from multiple industries.

## 2.2. The MerPAS<sup>®</sup> and Its Preparation and Deployment in This Study

We used four to six MerPAS<sup>®</sup> units (Tekran Corp., Toronto, ON, Canada) to concurrently collect GEM at each site during each deployment (Figure 2). The development and performance characteristics of the passive sampler have been described in detail elsewhere [25,31,32]. Briefly, sulfur-impregnated activated carbon serves as a sorbent, and is housed in a stainless-steel mesh cylinder at the center of the device (Figure A1). The mesh is inserted into a microporous diffusive barrier (white Radiello<sup>®</sup>, Sigma Aldrich, St. Louis, MO, USA) which constrains the sampling rate. GEM diffuses through the barrier and is retained on the sorbent, but GOM and PBM do not appreciably pass the barrier [33]. The diffusive barrier itself is screwed into the center of a protective shield that permits outdoor deployment. The shield has an opening at the bottom that allows for air circulation but keeps precipitation out.

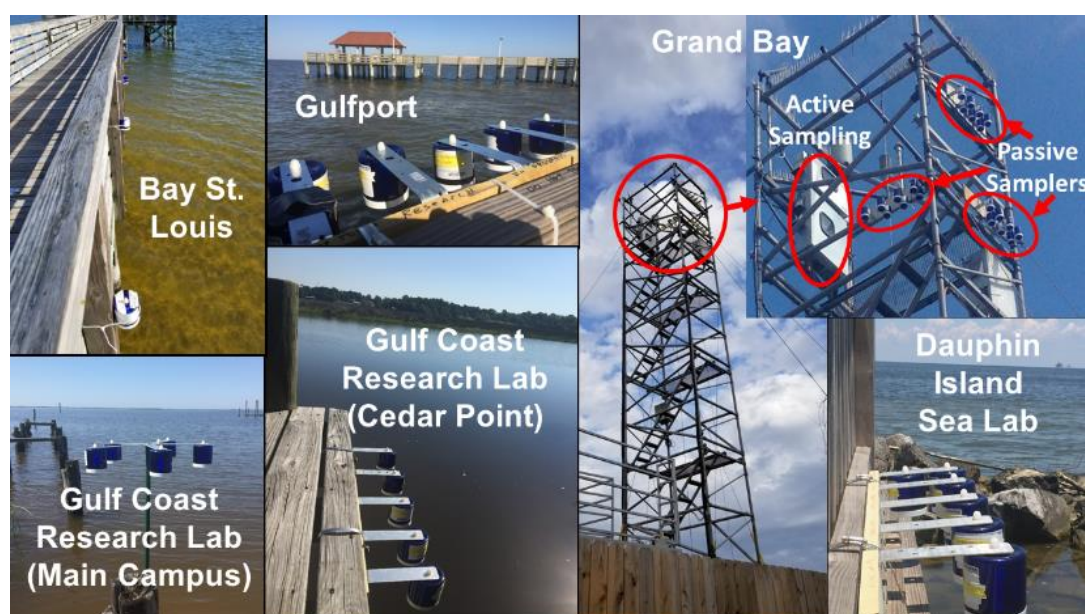


**Figure 2.** Views of the six sampling sites along the northern Gulf of Mexico (nGoM) showing deployment of passive air samplers for GEM collection.

In this study, we loaded about 0.6 g of freshly crushed and sieved (250–1000  $\mu\text{m}$ ) sulfur-impregnated activated carbon sorbent (HGR-AC, Calgon Carbon Corp., Pittsburg, PA, USA) into the samplers <3 days prior to deployment. Before loading the samplers, the activated carbon was analyzed for Hg to ascertain the blank level; the sorbent was only used when it would contribute <0.15 ng of Hg per sampler, amounting to <4% of the Hg accumulated during sampling. Samplers were deployed at 1.5 to 3.0 m above the water to prevent water from splashing into the device, except at Grand Bay where they were deployed at the top of a 10 m tower. We did not observe any salt inside the samplers and do not suspect water splashed into them. After each use, we cleaned diffusive barriers with a stream of nitrogen, and would only re-use them if they remained clean and undamaged; others have shown no significant difference in sampling rate between new and used barriers if the barriers are kept clean and in good condition [32].

## 2.3. Determination of Hg Collected on the Pas Sorbent and Calculation of Atmospheric Hg Concentrations

Upon retrieval the PASs were capped, sealed with polytetrafluoroethylene tape, placed in Ziplock bags, transported to the laboratory, and stored in a clean room until analysis within 2 days of collection. Details of the analysis were described in a previous study [28]. Briefly, total Hg collected on the sorbent was determined by a Direct Mercury Analyzer (DMA-80; Milestone Inc., Shelton, CT, USA), a technique which is based on thermal decomposition, gold amalgamation, and atomic absorption spectrometry. We followed U.S. Environmental Protection Agency (EPA) Method 7473, with some modifications for

trapping the sulfur released from the sulfur-impregnated activate carbon with  $\text{Na}_2\text{CO}_3$  [34]. Prior to analysis, quartz sample holders (boats) were pre-cleaned by soaking in 5% nitric acid overnight, rinsed with deionized water, and heated to 550 °C for several hours to remove any traces of Hg. Then the sorbent within the stainless-steel mesh cylinder was weighed into the boats and covered with ~0.2 g of  $\text{Na}_2\text{CO}_3$ . This process was repeated using a second boat because the capacity of a single boat was not enough for the amount of sorbent in a PAS. The boats were then loaded into the autosampler and analyzed by the DMA, with the Hg for the two boats being combined. The DMA instrument was calibrated using Hg solutions that were prepared from a 10  $\mu\text{g ml}^{-1}$  Hg stock solution (Spex Certiprep, Metuchen, NJ, USA). Coal fly ash standard reference material (SRM; NIST 1633C) was analyzed before beginning the sample analysis and every 20 boats thereafter. Recovery of SRM over the analyses was  $94.6 \pm 4.2\%$  (mean  $\pm$  SD,  $n = 16$ ). The limit of detection was 0.014 ng of Hg.

Concentrations of GEM were calculated by dividing the mass of adsorbed Hg (ng) by the deployment time (days) and the sampling rate ( $\text{m}^3 \text{ day}^{-1}$ ). Hg uptake (after blank subtraction) ranged from 3.14 to 4.58 ng during ~4 weeks deployment period. We used a sampling rate of 0.111  $\text{m}^3 \text{ day}^{-1}$  recommended by Tekran. The sampling rate was adjusted for local temperature and wind speed, factors which can influence the molecular diffusivity of GEM and the overall sampling rate, respectively [32]. Meteorological data are given in Table A1 in Appendix A. The adjusted sampling rate was calculated using Equation (1) [32] and ranged from 0.106 to 0.133 ( $\text{m}^3 \text{ day}^{-1}$ ), depending on season and location.

$$\text{SR}_{\text{adj.}} = \text{SR}_{\text{cal}} + (T - 9.89 \text{ }^\circ\text{C}) \cdot 0.0009 \text{ m}^3 (\text{day } ^\circ\text{C})^{-1} + (W - 3.41 \text{ m s}^{-1}) \cdot 0.003 \text{ m}^3 (\text{day } ^\circ\text{C})^{-1} \quad (1)$$

#### 2.4. Measurement of GEM at NOAA's Grand Bay Site Using Active Sampling

Atmospheric speciated mercury (GEM, GOM, and PBM) was monitored at the Grand Bay using a Tekran speciation system, which has been described elsewhere [12,17]. Briefly, ambient air is sampled by the mercury detection system at approximately 10 L/min. Large particles ( $d > 2.5 \mu\text{m}$ ) are removed at the inlet by an elutriator/impactor assembly, GOM is collected on a KCl-coated quartz annular denuder, and PBM ( $d < 2.5 \mu\text{m}$ ) is collected on a quartz regenerable particle filter (RPF). GEM passes through the glassware unimpeded and is sequentially collected on one of two gold traps at 5-min intervals. As one trap collects GEM, the other is heated to thermally desorb GEM into a flow of argon, and the liberated GEM is detected via cold vapor atomic fluorescence spectrometry. After one hour, sample collection ceases and the collected GOM on the denuder and PBM on the quartz filter are then sequentially thermally desorbed in a flow of mercury-free zero air and quantitatively converted to GEM, which is then analyzed by the mercury detector. Thus, the speciation system operates on a 50% duty cycle, and reports GEM in real time at 5-min intervals during the sampling hour, and one-hour integrated concentrations of GOM and PBM during the subsequent desorption cycle. AMNet standard operating protocols ([35], <http://nadp.slh.wisc.edu/AMNet/docs.aspx>) were followed for mercury measurement and data reduction. Herein we focus on the GEM data for comparison with our PAS data.

#### 2.5. Statistical Analysis

Differences in passively sampled GEM concentrations among locations and seasons and the interaction between location and season were examined using univariate repeated measures analysis of variance (rmANOVA). Location was treated as a between-subjects effect, whereas season and its interaction with location were treated as within-subjects effects. Given a significant main effect of location, Tukey's tests of honest significant differences (HSD tests) were used to examine pairwise differences in GEM means among locations. Pairwise differences among seasons were tested using t-tests and a Sidak  $p$ -value adjustment for multiple comparisons. The components of a significant season  $\cdot$  location interaction were tested using planned orthogonal contrasts. Contrasts were chosen to test the hypothesis that GEM concentrations were greater outside the growing season (winter) than during other times of the year, and lower during the hottest growing season (summer) than in the

spring and fall. Contrasts associated with the components of the season · location interaction included (1) the difference in GEM between winter and the remaining seasons depended on location ((winter v. rest) · location), (2) the difference in GEM between summer and the average of spring and fall depended on location ((summer v. spr/fall) · location), and (3) the difference in GEM between spring and fall depended on location ((spr v. sum) · location). Differences were deemed significant at a  $p < 0.05$  level.

Four one-sample t-tests (one for each season) were used to examine GEM concentration differences between active and passive sampling methods at Grand Bay NERR. Since the same active sampler was used to take hundreds of measurements in a given season, the measurements could not be considered independent observations. Hence, we averaged all actively sampled measurements in each season, assuming no replication and thus no within-season variation for the active sampler. We then compared the sample mean and standard error (SE, defined as the sample standard deviation (SD) divided by the  $\sqrt{n}$ ) of passively-sampled GEM concentrations for the deployment periods in each season to the average GEM concentration for the active sampler during the corresponding period. Although the one-sample t-tests assumed no statistical error, active samplers have an estimated 10% measurement error [16,17]. We therefore assumed that the seasonal average measurement of GEM by each active sampler represented the midpoint of this 10% measurement uncertainty interval. We corrected the  $p$ -values produced by each of the four one-sample t-tests using Sidak's multiplicative correction for multiple t-tests. Differences were deemed significant at a  $p < 0.05$  level. Data were analyzed using SYSTAT (version 13.0, San Jose, CA, USA).

### 3. Results and Discussion

Overall precision between the samplers deployed side-by-side averaged ~7% relative standard deviation, which is in the expected range for this method [31]. Adjustment of the sampling rate using local meteorological data generally decreased the GEM levels from 0–8%, except during the cold fall and winter periods where GEM increased at a few sites by up to 6%, and during July 2019 when a windy summer tropical storm helped decrease GEM levels by as much as 14% at Gulfport. Adjustments at Grand Bay were generally greater because it tended to be windier atop the 10 m tower.

#### 3.1. Seasonal Trends of GEM Concentration along the nGoM Using PASs

GEM concentrations ( $\text{ng m}^{-3}$ ) varied significantly among seasons (rmANOVA  $F_{\text{season } 3,75} = 107.58$ ; unadjusted and Greenhouse–Geisser  $p < 0.01$ ). Mean seasonal GEM concentrations ( $\text{ng m}^{-3} \pm 1 \text{ SE}$ ) at each of the six locations are shown in Figure 3, with specific values given in Table A2 in Appendix A. Mean concentrations ranged from  $1.00 \pm 0.03 \text{ ng m}^{-3}$  in the summer at GCRL Cedar Point to  $1.77 \pm 0.03 \text{ ng m}^{-3}$  in the winter at Bay St. Louis. Differences among seasons averaged across locations revealed that GEM concentrations were significantly higher in the winter than in all other seasons across all sites ( $1.53 \pm 0.03$  (winter),  $1.18 \pm 0.03$  (fall),  $1.25 \pm 0.03$  (spring), and  $1.14 \pm 0.02$  (summer); Sidak-adjusted  $p < 0.05$ ; Figure 3). GEM concentrations were lower in the summer than in spring (Sidak  $p < 0.01$ ; Figure 3), but not significantly lower than in fall (Sidak-adjusted  $p = 0.12$ ). There was no significant difference in GEM concentration between spring and fall (Sidak-adjusted  $p = 0.29$ ; Figure 3).

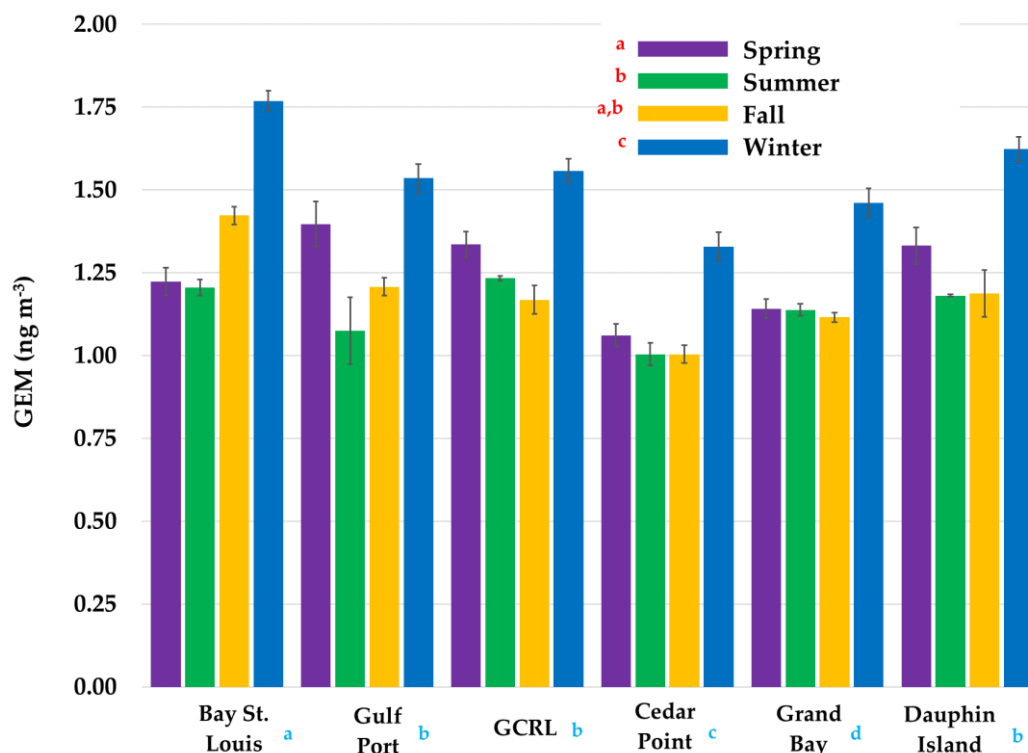


**Figure 3.** GEM concentrations determined using passive air samplers (PASs) deployed at six sites along the nGoM from May 2019 to February 2020. Sites are depicted west to east (from left to right) and error bars represent 1 standard error. Results for two sets of statistical analyses are shown: (1) pairwise means comparisons for the main effect of season (red letters), and (2) pairwise means comparisons for the main effect of location (blue letters). Seasons or locations that do not share letters are statistically different ( $p < 0.05$ ) as determined by Tukey's honest significant difference tests. The season  $\cdot$  location interaction is described in the text.

GEM levels tend to be higher in the winter due in part to the uptake of Hg by plants during the growing season which generally extends from spring through early fall [5], but also due to shifts in prevailing winds which are generally from the south (arriving from the GoM) in the summer and from the north (over terrestrial areas with point sources) in the winter (Figure A2) [16,17]. Other factors that can contribute to seasonal differences in atmospheric Hg species include greater sunlight intensity in the summer, which can increase conversion of GEM to GOM by photochemical oxidation, and precipitation in the summer from convective thunderstorms that can strip GOM from the air, resulting in high levels of wet Hg deposition [16,17,36]. Seasonal trends of airborne Hg species in southeastern U.S. have now been studied using both active and passive sampling, and our data are consistent with previously reported trends [16,37,38].

The pattern of seasonal differences in GEM concentrations varied among locations, as indicated by a significant season  $\times$  location interaction (rmANOVA  $F_{\text{season} \cdot \text{location}}(15,75) = 3.14$ ; unadjusted and Greenhouse–Geisser  $p < 0.01$ ). The difference in GEM between fall and spring varied among locations (Contrast  $F_{\text{fall v. spring} \cdot \text{location}}(5,25) = 3.14$ ;  $p = 0.03$ ). Whereas GEM in the fall was greater than GEM in the spring at Bay St. Louis, the same was not true at other locations (Figure 3). The difference in GEM between summer and the average of spring and fall varied significantly among locations (Contrast  $F_{\text{summer v. spr/fall} \cdot \text{location}}(5,25) = 4.12$ ;  $p < 0.01$ ). Whereas GEM was lower in the summer than the average for spring or fall at Bay St. Louis and Gulfport, this difference was lower at Dauphin Island, Cedar Point, and GCRL, and absent at Grand Bay (Figure 3). Spatial differences are examined further below.

### 3.2. Spatial Trends of GEM Concentration along the nGoM Using PASs

Previous studies have shown that coastal sites can be influenced by both polluted air from urban environments and cleaner Gulf of Mexico marine air [17,39]. In our study, GEM concentrations varied significantly among locations (rmANOVA  $F_{\text{location}(5,25)} = 38.60; p \ll 0.01$ ). Averaged across seasons, Tukey’s HSD tests revealed that GEM at Bay St. Louis was higher than at all other sites ( $p < 0.05$ ) (Figure 3). As the western-most site, Bay St. Louis is closest to New Orleans (<100 km), by far the largest population center in the area with a number of Hg sources from various industries. For the New Orleans and Baton Rouge area, Hg emissions in 2018 amounted to ~206 kg, more than double the amount emitted from all the sites in Mississippi shown in Figure 1. In addition, there is a close-in point source ~6 km to the north of the Bay St. Louis site (Figure 1). Generally there are higher GEM concentrations from the north and northeast during the winter and from the southwest during the summer for active sampling at the Grand Bay site (Figure 4). Detailed air mass back-trajectory and source-receptor modelling at each site is beyond the scope of this work. Additional study is needed to determine the persistence and cause of the higher GEM concentrations found at Bay St. Louis.

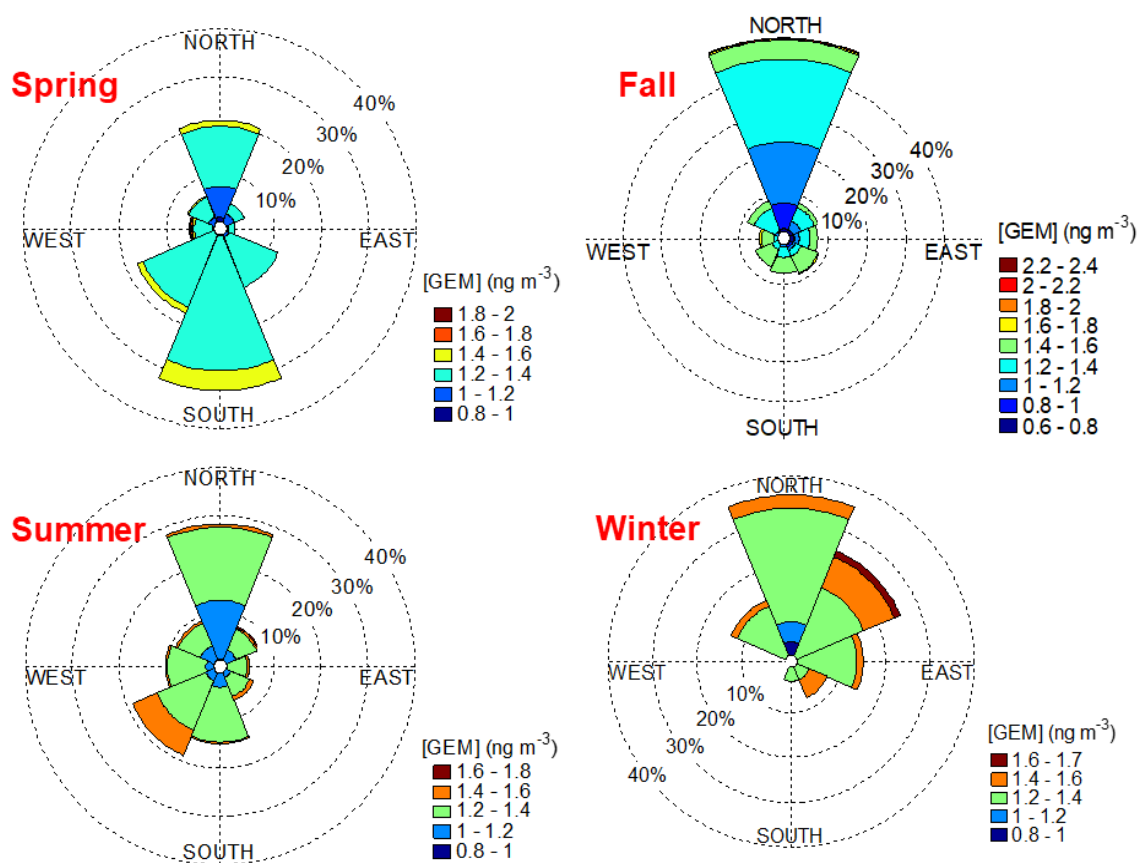


**Figure 4.** Wind roses showing the relationship between GEM levels and wind direction for each sampling period at Grand Bay.

We also observed the lowest GEM concentrations at the Cedar Point coastal marsh site (Figure 3). The site is located away from the coastal beach area in a sheltered Bayou and was in proximity to the most surrounding vegetation, a known sink for airborne Hg. The Grand Bay site is also within a wetland, but we sampled there from the top of the 10 m tower, likely capturing air masses relatively unimpeded by vegetation, which may have moderated the wetland effect. Tukey’s HSD tests revealed no statistical differences among the other open water coastal sites (Gulfport, GCRL Main Campus, and Dauphin Island;  $p > 0.83$ ). However, there are certainly additional complexities in this sub-tropical coastal environment that passive air samplers are unable to resolve given their long deployment times.

For example, although GOM data is not included herein, GOM concentrations at coastal sites can be influenced not only by regional point sources [16], but by conversion of GEM to GOM through photochemical oxidation associated with halogen species, such as BrO and BrCl, derived from marine aerosols [40–42].

### 3.3. Comparison of GEM Determined by Cctive and Passive Sampling at Grand Bay

Compared to passive sampling, active sampling provides high temporal resolution with many more data points. At Grand Bay, we observed diurnal variations, seasonal trends, unknown plume events, and other complexity (Figure A3). Detailed analysis of Hg species fluctuations is beyond the scope of this study, but others have reported on this in the region [16,39,43]. Here, we focus on preliminary data comparing GEM concentrations between passive and active sampling techniques for data co-collected at the AMNet Grand Bay NERR site. It is worth mentioning that GEM levels have been declining at the Grand Bay site at a rate of  $-0.009 \text{ ng m}^{-3}/\text{yr}$  from 2007–2018, which may be partly explained by a concurrent decrease in anthropogenic Hg emissions in the region, especially for the electric power generating industry [16,29].

Summary statistics for GEM concentrations determined at Grand Bay are given in Table A3 in Appendix A. We observed similar seasonal trends in GEM concentration with highest concentrations in winter by both active and passive sampling methods. However, active sampling gave slightly higher mean GEM concentrations in the spring, summer, and fall, but not in the winter (one-sample  $t_{(\text{passive-active})} = -5.16, -7.13, -10.66, \text{ and } 1.43$  for spring, summer, fall, and winter, respectively, with  $df = 5, 5, 11, \text{ and } 5$ ; Figure 5). The trend is also depicted in Figure A3. It is unclear why passive sampling gave slightly lower average concentrations compared to active sampling for the spring, summer, and fall, and why winter was the exception. The re-use of the passive samplers may have caused a small bias or the activated carbon stock may have changed in some way over time, although it was still analyzed prior to analyses for blank subtraction. Nevertheless, the <15% difference between the averages of the two methods, operated by two different groups, may be considered acceptable, especially when evaluating larger spatial and temporal trends.

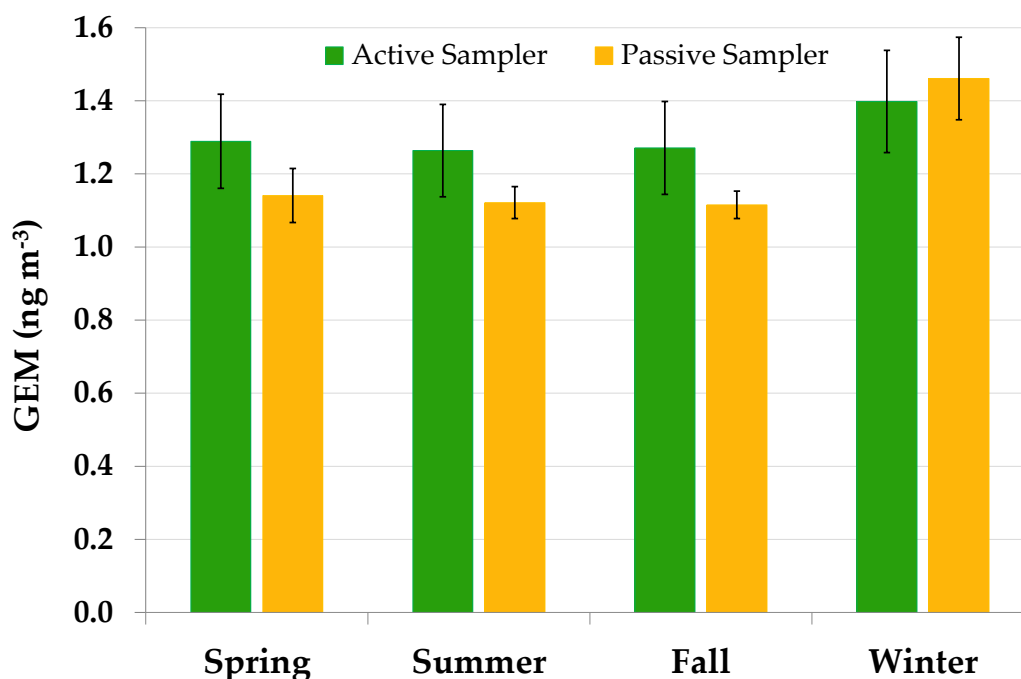


**Figure 5.** GEM concentrations determined using passive and active sampling at Grand Bay NERR. Error bars for passive sampler data represent 95% confidence intervals. Bars for the active sampler data represent 10% measurement error.

#### 4. Conclusions

We deployed MerPAS<sup>®</sup> passive air samplers to determine GEM at multiple sites along the nGoM over the course of a year. We observed higher GEM levels in the winter compared to other seasons across the sites. Spatially, mean GEM levels were highest at Bay St. Louis, the western-most site nearest New Orleans, and lowest at Cedar Point, a coastal marsh site with extensive vegetation. MerPAS<sup>®</sup> units were also deployed at Grand Bay near a Tekran air Hg speciation system that is based on active sampling. The passive air samplers gave slightly lower concentrations to the active sampling method, except in the winter. Despite the difference, the MerPAS<sup>®</sup> passive air samplers were capable of discriminating both seasonal and spatial differences, providing further insight into the sources and factors that influence GEM along the nGoM.

**Author Contributions:** J.V.C. conceptualized, supervised, and administered the project; B.J. led the P.A.S. sampling and measurement campaign; J.S.B. and B.J. provided statistical analyses; B.J. and J.V.C. prepared the original draft; X.R., P.K. and W.T.L. provided the Grand Bay active sampling data; M.D.C. prepared Figure 1; X.R. prepared the wind rose plots. All authors helped review and edit the paper. All authors have read and agreed to the published version of the manuscript.

**Funding:** This research was funded by seed grants from the Mississippi Space Grant Consortium and RII Track-2 FEC: Emergent Polymer Sensing Technologies for Gulf Coast Water Quality Monitoring, which was part of NSF Award #1632825.

**Acknowledgments:** We thank those who gave us permission to deploy our PASs at our sampling sites. We are particularly grateful to Mike Archer at the Grand Bay NERR for access to the AMNet tower and help with sampling. We are also thankful to Eric Prestbo, Lucas Hawkins, Diana Babi, and others at Tekran Corp. for their continued advice and support.

**Conflicts of Interest:** The authors declare no conflict of interest.

## Appendix A

**Table A1.** Coordinates for sampling sites and nearest weather stations, along with sampling periods and mean temperature and wind speed during deployment.

	Bay St. Louis		Gulf Port		GCRL (Main Campus)		GCRL (Cedar Point)		Grand Bay		Dauphin Island	
Deployment Sites:	30.302°N, 89.327°W		30.361°N, 89.083°W		30.392°N, 88.799°W		30.392°N, 88.775°W		30.412°N, 88.404°W		30.251°N, 88.077°W	
Weather Stations:	30.287°N, 89.376°W		30.364°N, 89.086°W		30.401°N, 88.808°W		30.401°N, 88.773°W		30.412°N, 88.404°W		30.254°N, 88.103°W	
Sampling Period	Temp. (°C)	Wind (m/s)	Temp. (°C)	Wind (m/s)	Temp. (°C)	Wind (m/s)	Temp. (°C)	Wind (m/s)	Temp. (°C)	Wind (m/s)	Temp. (°C)	Wind (m/s)
May–June (16/5/2019–13/6/2019)	27.0	1.6	27.0	5.7	27.2	0.3	26.4	0.9	26.7	3.0	27.2	1.0
June–July (13/6/2019–11/7/2019)	28.1	1.4	28.5	4.7	28.7	0.3	27.9	0.9	27.9	2.9	28.7	1.2
July–August (11/7/2019–8/8/2019)	26.8	1.3	26.4	4.9	27.4	0.3	26.8	0.8	26.7	2.2	28.3	1.1
August–September (8/8/2019–5/9/2019)	27.4	0.8	28.4	3.5	27.5	0.2	27.1	0.4	27.4	1.8	28.5	0.9
November–December (1/11/2019–3/12/2019)	12.8	1.0	13.7	3.6	13.0	0.5	13.0	0.5	13.4	2.3	14.9	2.1
January–February (27/1/2020–18/2/2020)	13.7	1.3	14.3	4.6	14.3	0.7	14.3	1.1	14.8	4.9	14.6	2.1

**Table A2.** Amount of Hg (ng) collected on each PAS and GEM concentrations based on those amounts ( $n = 6$ , unless otherwise noted).

Sampling Period	Amount of Hg Collected and GEM Level	Bay St. Louis		Gulf Port		GCRL Main Campus		GCRL Cedar Point		Grand Bay		Dauphin Island		All Locations	
		Mean	SE	Mean	SE	Mean	SE	Mean	SE	Mean	SE	Mean	SE	Mean	SE
16/5/2019–13/6/2019	Hg (ng)	4.12 <sup>a</sup>	0.14	4.60	0.22	4.54	0.13	3.64	0.12	4.00	0.11	4.48	0.19	4.23	0.15
	Conc. (ng m <sup>-3</sup> )	1.22	0.04	1.40	0.07	1.34	0.04	1.06	0.03	1.14	0.03	1.33	0.06	1.25	0.03
13/6/2019–11/7/2019	Hg (ng)	3.77 <sup>b</sup>	0.09	3.90	0.08	3.95	0.17	3.45 <sup>a</sup>	0.13	3.77	0.12	3.85	0.06	3.78	0.07
	Conc. (ng m <sup>-3</sup> )	1.15	0.03	1.10	0.02	1.24	0.05	1.06	0.04	1.11	0.04	1.18	0.02	1.14	0.02
11/7/2019–8/8/2019	Hg (ng)	Lost in tropical storm		3.36	0.21	4.07	0.11	3.14 <sup>a</sup>	0.06	4.00	0.16	3.98 <sup>a</sup>	0.12	3.71	0.70
	Conc. (ng m <sup>-3</sup> )			0.89	0.05	1.24	0.03	0.95	0.02	1.17	0.05	1.18	0.04	1.09	0.05
8/8/2019–5/9/2019	Hg (ng)	4.19 <sup>a</sup>	0.07	4.29	0.06	3.95	0.10	3.25	0.21	3.98	0.07	4.11	0.02	3.96	0.15
	Conc. (ng m <sup>-3</sup> )	1.26	0.02	1.24	0.02	1.22	0.03	1.00	0.06	1.13	0.02	1.19	0.01	1.17	0.02
1/11/2019–3/12/2019	Hg (ng)	4.36 <sup>a</sup>	0.08	4.43 <sup>a</sup>	0.10	3.92 <sup>a</sup>	0.14	3.37 <sup>a</sup>	0.09	3.96	0.05	4.26	0.25	4.05	0.16
	Conc. (ng m <sup>-3</sup> )	1.42	0.03	1.21	0.03	1.17	0.04	1.00	0.03	1.12	0.01	1.19	0.07	1.18	0.03
27/1/2020–18/2/2020	Hg (ng)	4.58 <sup>b</sup>	0.08	4.35	0.12	4.17	0.10	3.60	0.12	4.42	0.13	4.50	0.10	4.27	0.15
	Conc. (ng m <sup>-3</sup> )	1.77	0.03	1.54	0.04	1.56	0.04	1.33	0.04	1.46	0.04	1.62	0.04	1.53	0.03
All Seasons	Hg (ng)	4.21	0.07	4.15	0.09	4.10	0.06	3.42	0.06	4.02	0.05	4.20	0.07		
	Conc. (ng m <sup>-3</sup> )	1.36	0.05	1.23	0.04	1.29	0.03	1.07	0.09	1.19	0.02	1.28	0.03		

<sup>a</sup> $n = 5$ ; <sup>b</sup> $n = 4$ . SE = Standard Error

**Table A3.** Summary statistics for GEM concentrations at Grand Bay NERR by active and passive sampling along with meteorological data used to obtain the adjusted sampling rate for each PAS.

Season	Mean Temperature (°C)	Mean Wind Speed (m/s)	Statistical Parameter	Active Sampler (ng m <sup>-3</sup> )	Passive Sampler (ng m <sup>-3</sup> )
Spring 2019	26.7	3.0	n	324	6
			Range	0.90–1.81	1.07–1.27
			Mean	1.29	1.14
			Median	1.30	1.14
			SD	0.10	0.07
Summer 2019	27.3	2.5	n	550	18
			Range	0.98–1.64	1.03–1.38
			Mean	1.26	1.14
			Median	1.26	1.12
			SD	0.10	0.09
Fall 2019	13.4	2.3	n	371	6
			Range	0.71–1.68	1.06–1.15
			Mean	1.27	1.12
			Median	1.30	1.12
			SD	0.20	0.04
Winter 2020	14.8	4.9	n	256	6
			Range	0.89–1.66	1.35–1.64
			Mean	1.40	1.46
			Median	1.39	1.43
			SD	0.14	0.11

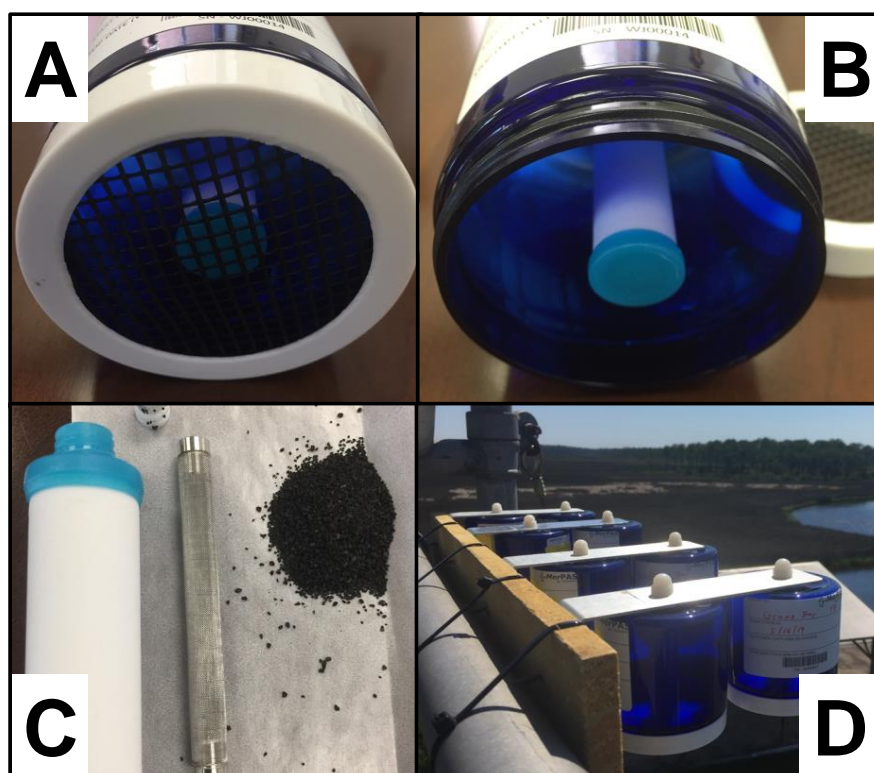


**Figure A1.** Photos showing the MerPAS<sup>®</sup> configuration with cover on (A), with the cover off (B), and with diffusive body, stainless steel screen, and activated carbon sorbent removed (C), and deployment on the tower at Grand Bay (D).

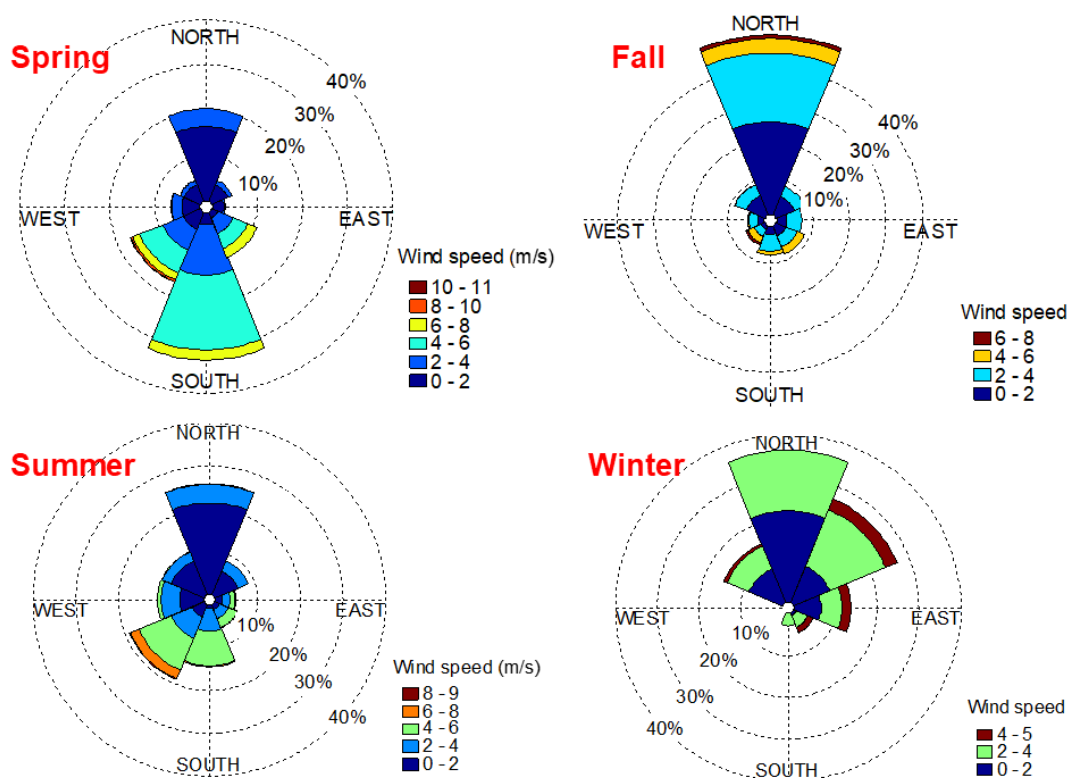


Figure A2. Wind roses showing the relationship between wind speed and wind direction for each sampling period at Grand Bay.

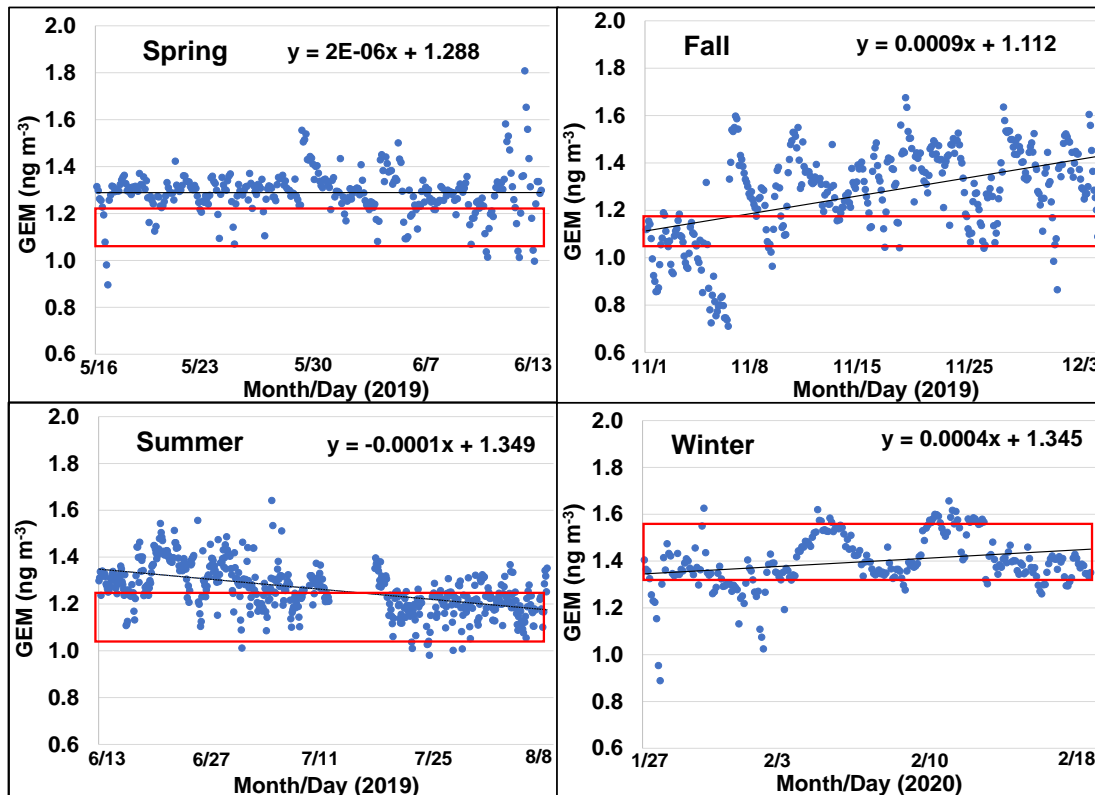


Figure A3. Hourly GEM concentrations determined at the Grand Bay NERR site using active sampling. The red box encompasses the passive sampler data (average  $\pm$  1SD) obtained for the same period. The equation is for the linear regression of the data with the trend line in black.

## References

1. Fitzgerald, W.F.; Engstrom, D.R.; Mason, R.P.; Nater, E.A. The Case for Atmospheric Mercury Contamination in Remote Areas. *Environ. Sci. Technol.* **1998**, *32*, 1–7. [[CrossRef](#)]
2. Gustin, M.; Jaffe, D. Reducing the Uncertainty in Measurement and Understanding of Mercury in the Atmosphere. *Environ. Sci. Technol.* **2010**, *44*, 2222–2227. [[CrossRef](#)] [[PubMed](#)]
3. Lyman, S.N.; Cheng, I.; Gratz, L.E.; Weiss-Penzias, P.; Zhang, L. An updated review of atmospheric mercury. *Sci. Total Environ.* **2020**, *707*, 135575. [[CrossRef](#)] [[PubMed](#)]
4. Gustin, M.S.; Amos, H.M.; Huang, J.; Miller, M.B.; Heidecorn, K. Measuring and modeling mercury in the atmosphere: A critical review. *Atmos. Chem. Phys.* **2015**, *15*, 5697–5713. [[CrossRef](#)]
5. Schroeder, W.H.; Munthe, J. Atmospheric mercury—An overview. *Atmos. Environ.* **1998**, *32*, 809–822. [[CrossRef](#)]
6. Driscoll, C.T.; Mason, R.P.; Chan, H.M.; Jacob, D.J.; Pirrone, N. Mercury as a Global Pollutant: Sources, Pathways, and Effects. *Environ. Sci. Technol.* **2013**, *47*, 4967–4983. [[CrossRef](#)] [[PubMed](#)]
7. Lin, C.-J.; Pehkonen, S.O. The chemistry of atmospheric mercury: A review. *Atmos. Environ.* **1999**, *33*, 2067–2079. [[CrossRef](#)]
8. Sprovieri, F.; Pirrone, N.; Bencardino, M.; D'Amore, F.; Carbone, F.; Cinnirella, S.; Mannarino, V.; Landis, M.; Ebinghaus, R.; Weigelt, A.; et al. Atmospheric mercury concentrations observed at ground-based monitoring sites globally distributed in the framework of the GMOS network. *Atmos. Chem. Phys.* **2016**, *16*, 11915–11935. [[CrossRef](#)]
9. Zhang, Y.; Jacob, D.J.; Horowitz, H.M.; Chen, L.; Amos, H.M.; Krabbenhoft, D.P.; Slemr, F.; St. Louis, V.L.; Sunderland, E.M. Observed decrease in atmospheric mercury explained by global decline in anthropogenic emissions. *Proc. Natl. Acad. Sci. USA* **2016**, *113*, 526–531. [[CrossRef](#)]
10. Choi, A.L.; Grandjean, P. Methylmercury exposure and health effects in humans. *Environ. Chem.* **2008**, *5*, 112–120. [[CrossRef](#)]
11. Hall, B.D.; Aiken, G.R.; Krabbenhoft, D.P.; Marvin-DiPasquale, M.; Swarzenski, C.M. Wetlands as principal zones of methylmercury production in southern Louisiana and the Gulf of Mexico region. *Environ. Pollut.* **2008**, *154*, 124–134. [[CrossRef](#)] [[PubMed](#)]
12. Ren, X.; Luke, W.T.; Kelley, P.; Cohen, M.D.; Artz, R.; Olson, M.L.; Schmeltz, D.; Puchalski, M.; Goldberg, D.L.; Ring, A.; et al. Atmospheric mercury measurements at a suburban site in the Mid-Atlantic United States: Inter-annual, seasonal and diurnal variations and source-receptor relationships. *Atmos. Environ.* **2016**, *146*, 141–152. [[CrossRef](#)]
13. Engle, M.A.; Tate, M.T.; Krabbenhoft, D.P.; Kolker, A.; Olson, M.L.; Edgerton, E.S.; DeWild, J.F.; McPherson, A.K. Characterization and cycling of atmospheric mercury along the central US Gulf Coast. *Appl. Geochem.* **2008**, *23*, 419–437. [[CrossRef](#)]
14. Lincoln, R.A.; Shine, J.P.; Chesney, E.J.; Vorhees, D.J.; Grandjean, P.; Senn, D.B. Fish Consumption and Mercury Exposure among Louisiana Recreational Anglers. *Environ. Health Perspect.* **2011**, *119*, 245–251. [[CrossRef](#)]
15. Merritt, K.A.; Amirbahman, A. Mercury methylation dynamics in estuarine and coastal marine environments—A critical review. *Earth Sci. Rev.* **2009**, *96*, 54–66. [[CrossRef](#)]
16. Ren, X.; Luke, W.T.; Kelley, P.; Cohen, M.D.; Olson, M.L.; Walker, J.; Cole, R.; Archer, M.; Artz, R.; Stein, A.A. Long-Term Observations of Atmospheric Speciated Mercury at a Coastal Site in the Northern Gulf of Mexico during 2007–2018. *Atmosphere* **2020**, *11*, 268. [[CrossRef](#)]
17. Ren, X.; Luke, W.; Kelley, P.; Cohen, M.; Ngan, F.; Artz, R.; Walker, J.; Brooks, S.; Moore, C.; Swartzendruber, P.; et al. Mercury Speciation at a Coastal Site in the Northern Gulf of Mexico: Results from the Grand Bay Intensive Studies in Summer 2010 and Spring 2011. *Atmosphere* **2014**, *5*, 230–251. [[CrossRef](#)]
18. Rolison, J.M.; Landing, W.M.; Luke, W.; Cohen, M.; Salters, V.J.M. Isotopic composition of species-specific atmospheric Hg in a coastal environment. *Chem. Geol.* **2013**, *336*, 37–49. [[CrossRef](#)]
19. Pandey, S.K.; Kim, K.-H.; Brown, R.J.C. Measurement techniques for mercury species in ambient air. *TrAC Trends Anal. Chem.* **2011**, *30*, 899–917. [[CrossRef](#)]
20. Gustin, M.S.; Lyman, S.N.; Kilner, P.; Prestbo, E. Development of a passive sampler for gaseous mercury. *Atmos. Environ.* **2011**, *45*, 5805–5812. [[CrossRef](#)]

21. Skov, H.; Sørensen, B.T.; Landis, M.S.; Johnson, M.S.; Sacco, P.; Goodsite, M.E.; Lohse, C.; Christiansen, K.S. Performance of a new diffusive sampler for Hg<sup>0</sup> determination in the troposphere. *Environ. Chem.* **2007**, *4*, 75–80. [[CrossRef](#)]
22. Brumbaugh, W.G.; Petty, J.D.; May, T.W.; Huckins, J.N. A passive integrative sampler for mercury vapor in air and neutral mercury species in water. *Chemosphere Glob. Change Sci.* **2000**, *2*, 1–9. [[CrossRef](#)]
23. Peterson, C.; Alishahi, M.; Gustin, M.S. Testing the use of passive sampling systems for understanding air mercury concentrations and dry deposition across Florida, USA. *Sci. Total Environ.* **2012**, *424*, 297–307. [[CrossRef](#)] [[PubMed](#)]
24. Lyman, S.N.; Gustin, M.S.; Prestbo, E.M. A passive sampler for ambient gaseous oxidized mercury concentrations. *Atmos. Environ.* **2010**, *44*, 246–252. [[CrossRef](#)]
25. McLagan, D.S.; Mitchell, C.P.J.; Huang, H.; Lei, Y.D.; Cole, A.S.; Steffen, A.; Hung, H.; Wania, F. A High-Precision Passive Air Sampler for Gaseous Mercury. *Environ. Sci. Technol. Lett.* **2016**, *3*, 24–29. [[CrossRef](#)]
26. Szponar, N.; McLagan, D.S.; Kaplan, R.J.; Mitchell, C.P.J.; Wania, F.; Steffen, A.; Stuppel, G.W.; Monaci, F.; Bergquist, B.A. Isotopic Characterization of Atmospheric Gaseous Elemental Mercury by Passive Air Sampling. *Environ. Sci. Technol.* **2020**, *54*, 10533–10543. [[CrossRef](#)] [[PubMed](#)]
27. McLagan, D.S.; Monaci, F.; Huang, H.; Lei, Y.D.; Mitchell, C.P.J.; Wania, F. Characterization and Quantification of Atmospheric Mercury Sources Using Passive Air Samplers. *J. Geophys. Res. Atmos.* **2019**, *124*, 2351–2362. [[CrossRef](#)]
28. Jeon, B.; Cizdziel, J.V. Can the MerPAS Passive Air Sampler Discriminate Landscape, Seasonal, and Elevation Effects on Atmospheric Mercury? A Feasibility Study in Mississippi, USA. *Atmosphere* **2019**, *10*, 617. [[CrossRef](#)]
29. USEPA. Toxic Release Inventory. 2020. Available online: <https://www.epa.gov/toxics-release-inventory-triprogram/tri-basic-data-files-calendar-years-1987-2018> (accessed on 13 January 2020).
30. ESRI. *USA National Land Cover Database 2011, Based on Data from the Multi-Resolution Land Characteristics Consortium*; ESRI ArcGIS Data Server: Redlands, CA, USA, 2019.
31. McLagan, D.S.; Mitchell, C.P.J.; Steffen, A.; Hung, H.; Shin, C.; Stuppel, G.W.; Olson, M.L.; Luke, W.T.; Kelley, P.; Howard, D.; et al. Global evaluation and calibration of a passive air sampler for gaseous mercury. *Atmos. Chem. Phys.* **2018**, *18*, 5905–5919. [[CrossRef](#)]
32. McLagan, D.S.; Mitchell, C.P.J.; Huang, H.; Abdul Hussain, B.; Lei, Y.D.; Wania, F. The effects of meteorological parameters and diffusive barrier reuse on the sampling rate of a passive air sampler for gaseous mercury. *Atmos. Meas. Tech.* **2017**, *10*, 3651–3660. [[CrossRef](#)]
33. Stuppel, G.; McLagan, D.; Steffen, A. In situ reactive gaseous mercury uptake on radiello diffusive barrier, cation exchange membrane and teflon filter membranes during atmospheric mercury depletion events. In Proceedings of the 14th International Conference on Mercury as a Global Pollutant (ICMGP), Krakow, Poland, 8–13 September 2019.
34. McLagan, D.S.; Huang, H.; Lei, Y.D.; Wania, F.; Mitchell, C.P. Application of sodium carbonate prevents sulphur poisoning of catalysts in automated total mercury analysis. *Spectrochim. Acta Part B Spectrosc.* **2017**, *133*, 60–62. [[CrossRef](#)]
35. Gay, D.A.; Schmeltz, D.; Prestbo, E.; Olson, M.; Sharac, T.; Tordon, R. The Atmospheric Mercury Network: Measurement and initial examination of an ongoing atmospheric mercury record across North America. *Atmos. Chem. Phys.* **2013**, *13*, 11339–11349. [[CrossRef](#)]
36. National Atmospheric Deposition Program/Mercury Deposition Network. Available online: <http://nadp.slh.wisc.edu> (accessed on 24 September 2020).
37. Nair, U.S.; Wu, Y.; Walters, J.; Jansen, J.; Edgerton, E.S. Diurnal and seasonal variation of mercury species at coastal-suburban, urban, and rural sites in the southeastern United States. *Atmos. Environ.* **2012**, *47*, 499–508. [[CrossRef](#)]
38. Sexauer Gustin, M.; Weiss-Penzias, P.S.; Peterson, C. Investigating sources of gaseous oxidized mercury in dry deposition at three sites across Florida, USA. *Atmos. Chem. Phys.* **2012**, *12*, 9201–9219. [[CrossRef](#)]
39. Griggs, T.; Liu, L.; Talbot, R.W.; Torres, A.; Lan, X. Comparison of atmospheric mercury speciation at a coastal and an urban site in Southeastern Texas, USA. *Atmosphere* **2020**, *11*, 73. [[CrossRef](#)]
40. Sigler, J.M.; Mao, H.; Sive, B.C.; Talbot, R. Oceanic influence on atmospheric mercury at coastal and inland sites: A springtime nor'easter in New England. *Atmos Chem Phys* **2009**, *9*, 4023–4030. [[CrossRef](#)]

41. Coburn, S.; Dix, B.; Edgerton, E.; Holmes, C.D.; Kinnison, D.; Liang, Q.; ter Schure, A.; Wang, S.; Volkamer, R. Mercury oxidation from bromine chemistry in the free troposphere over the southeastern US. *Atmos. Chem. Phys.* **2016**, *16*, 3743–3760. [[CrossRef](#)]
42. Hedgecock, I.M.; Pirrone, N. Chasing Quicksilver: Modeling the Atmospheric Lifetime of Hg in the Marine Boundary Layer at Various Latitudes. *Environ. Sci. Technol.* **2004**, *38*, 69–76. [[CrossRef](#)]
43. Yi, J.; Cizdziel, J.; Lu, D. Temporal patterns of atmospheric mercury species in northern Mississippi during 2011–2012: Influence of sudden population swings. *Chemosphere* **2013**, *93*, 1694–1700. [[CrossRef](#)]



© 2020 by the authors. Licensee MDPI, Basel, Switzerland. This article is an open access article distributed under the terms and conditions of the Creative Commons Attribution (CC BY) license (<http://creativecommons.org/licenses/by/4.0/>).